IEEE Photonics Journal
An IEEE Photonics Society Publication

Open Access

A Method for Maintaining the Stability of Range Walk Error in Photon Counting Lidar With Probability Distribution Regulator

Volume 11, Number 6, December 2019

Jiaheng Xie
Zijing Zhang
Qunsong He
Jiahuan Li
Yuan Zhao

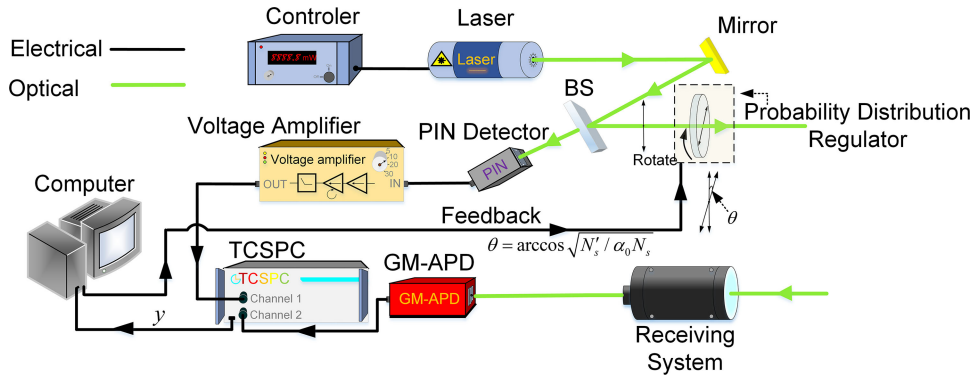

DOI: 10.1109/JPHOT.2019.2951111

A Method for Maintaining the Stability of Range Walk Error in Photon Counting Lidar With Probability Distribution Regulator

Jiaheng Xie, Zijing Zhang, Qunsong He, Jiahuan Li, and Yuan Zhao

School of Physics, Harbin Institute of Technology, Harbin 150001, China

DOI:10.1109/JPHOT.2019.2951111

Manuscript received October 23, 2019; accepted October 29, 2019. Date of publication November 4, 2019; date of current version December 16, 2019. This work was supported by the National Natural Science Foundation of China under Grant 61701139. Corresponding author: Yuan Zhao (e-mail: zhaoyuan@hit.edu.cn).

Abstract: Photon counting Lidar applied to long-distance ranging will face the problem of the number of received photons fluctuating with target distance and reflectivity. The Poisson probability model indicates that the range walk error of the system fluctuates with the number of received photons, which deteriorates the performance of ranging. We propose a novel approach based on the probability distribution regulator with feedback mechanism to achieve small and stable range walk error by actively controlling the number of photons incident on the detector. In this method, the attenuation rate of the probability distribution regulator varies with the number of photons to ensure that the number of photons incident on the detector is a fixed value. The simulated and experimental results with the approach demonstrate that ranging accuracy is improved significantly, and the stability of the range walk error is guaranteed.

Index Terms: GM-APD, photon counting, range walk error, lidar.

1. Introduction

With photon-level sensitivity and picosecond-level timing accuracy, the great capability to give accurate depth information of 3D scene makes lidar widely used. Applications such as remote sensing, weapon guidance, autonomous vehicles and target recognition are the most popular applications of lidar [1]–[5]. Time correlated single photon counting (TCSPC) technology is the most commonly used method to obtain flight time in pulse ranging lidar, while Geiger-mode avalanche photodiode (GM-APD) is often used in conjunction with TCSPC module due to its high single-photon sensitivity. In practical application, the ranging error stability is a critical index for photon counting lidar to achieve long-range and high-precision measurement. After analyzing the influencing factors of range walk error, compared to the target shape, detector quantum efficiency and background noise, the received laser intensity and pulse width are considered to be more important factors affecting range walk error [6]–[8]. Current researches mainly focus on reducing the range walk error caused by the fluctuation in number of photoelectrons, which can be divided into two aspects: algorithm recovery and system improvement. A Gaussian functions fitting method is used for restraint of range walk error [9]. Similarly, on the basis of a prior model, a numerical fitting method for range walk error and signal response rate is proposed to compensate for range walk error [10]. Xu *et al.* presented a signal restoration method to reduce the range walk error by correcting the difference

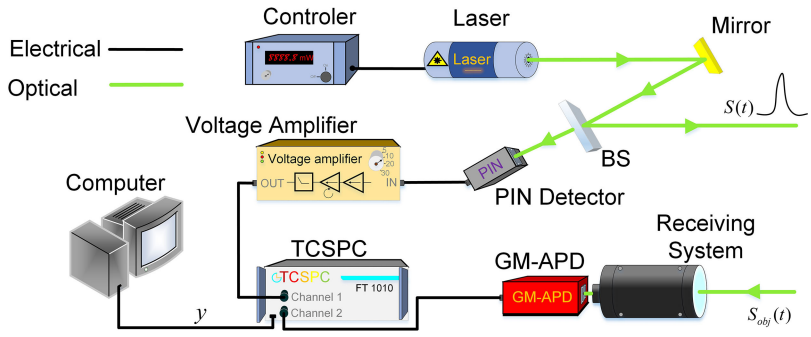

Fig. 1. A typical photon counting lidar system.

between photon counts and photoelectron distribution [11]. The system improvement measures include adding integrated current buffer [12], [13], short pulse pickup network [14] and unequally dual detection [15].

All of the above studies aim to reduce the range walk error, but there will still be fluctuations in the range walk error, which still deteriorate the ranging performance of the system. In this paper, the observation model for photon counting lidar based on Poisson probability distribution is deduced. We propose a novel probability distribution regulator method to control the number of photons incident on the GM-APD as a fixed value to reduce and stabilize range walk error. The simulation and experiment results have shown that our method effectively guarantees the stability of range walk error. For example, the standard deviation of ranging accuracy is reduced from 12.43 cm to 0.65 cm, and the standard deviation of ranging precision is reduced from 0.51 cm to 0.1 cm.

2. Theoretical Analysis

2.1 System Model

Fig. 1 shows a typical photon counting lidar system. A laser send a train of light pulses onto the beam splitter (BS) with the pulse waveform function $S(t)$. The light path is divided into two paths, one of which illuminates the target directly, the other is received by the high-speed PIN detector and converted into the start signal of TCSPC module. The receiving system collects the echo signal $S_{obj}(t)$ from the surface of the object and converges it on the Geiger APD detector surface. TCSPC module receives stop signal from GM-APD and build up photon arrival time histogram y. The depth R of the target can be calculated by several different algorithms from the histogram.

Consider a Gauss-shaped laser pulse:

$$S(t) = \frac{E_t}{h\nu}\frac{1}{\sigma_l\sqrt{2\pi}}e^{-\frac{t^2}{2\sigma_l^2}} \tag{1}$$

According to the radar equation, the number of photoelectrons at time t can be expressed as:

$$N_{sn}(t) = \frac{E_t}{h\nu}\frac{A_R}{2\pi R^2}\frac{\rho\eta_D\eta_R}{\sigma\sqrt{2\pi}}e^{-\frac{\left(t-\frac{2R}{c}\right)^2}{2\sigma^2}} + \eta_D N_b + N_d \tag{2}$$

Where E_t is single laser pulse energy. h and ν are respectively the Planck constant and laser frequency. The total average number of photons in a laser pulse is $E_t/h\nu$. The area and transmittance of the receiving system are A_R and η_R.The target with reflectivity ρ is located at distance R. c is the speed of light. η_D is detector quantum efficiency at ν. N_b and N_d are the number of background noise photoelectrons and darkcount noise photoelectrons at time t within a laser cycle.

Approximate the number of photoelectrons with a sampling period of Δt:

$$N_{sn}(i) = \int_{(i-1)\Delta t}^{i\Delta t} N_{sn}(t)dt \tag{3}$$

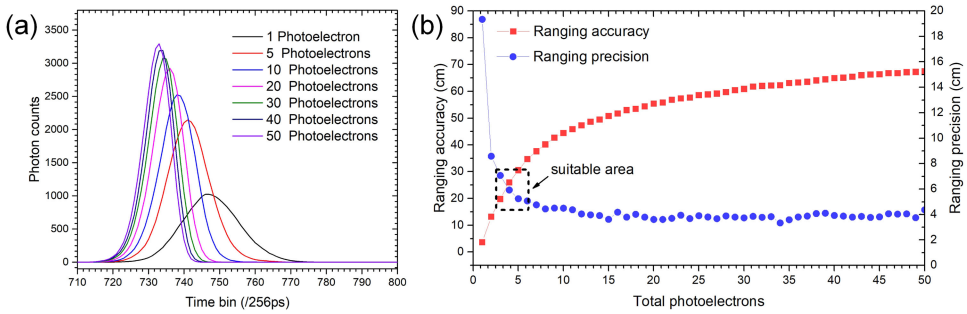

Fig. 2. (a) Simulated time histograms versus signal photoelectrons number. (b) Ranging error versus total signal photoelectrons.

Where Δt is the width of TCPSC module time bin. According to the Poisson probability response model of Gm-APD [16], the detection probability on the i-th time bin is presented as

$$P(i) = e^{-\sum_{j=1}^{i-1} N_{sn}(j)} \left[1 - e^{-N_{sn}(i)}\right] \tag{4}$$

A total of m laser pulses were emitted in TCSPC integration time so the mean of the TCSPC counts on the i-th time bin is

$$\bar{y}(i) = mP(i) = me^{-\sum_{j=1}^{i-1} N_{sn}(j)} \left[1 - e^{-N_{sn}(i)}\right] \tag{5}$$

2.2 Discrimination Method and Ranging Error

The center-of-mass method and the maximum position method are the two most commonly used algorithms to calculate the distance of the target from the histogram. Center-of-mass method is superior in the case of fewer statistics, while maximum position method is simple and fast. Here we use the center-of-mass method to obtain the target distance. For a sample $y(i)$ with mean of $\bar{y}(i)$ and m sampling times. The depth calculated by center-of-mass method is

$$R_{\text{com}} = \frac{c\Delta t}{2} \frac{\sum_{i=1}^{K} iy(i)}{\sum_{i=1}^{K} y(i)} \tag{6}$$

Where K is the number of time bins.

Accuracy and precision are two major indicators used to evaluate the ranging error. The former describes systematic errors and the latter represents random errors [8]. The standard deviation used to characterize the single-shot precision is called ranging precision error. It is expressed as

$$\sigma_{\text{precision}} = \sqrt{\frac{1}{N} \sum_{i=1}^{N} \left(R_i - \bar{R}\right)^2} \tag{7}$$

Where R_i is the $i-$th measurement, $\bar{R}$ is mean of N times measurements.

Ranging accuracy error measures the difference between measured value and real value, which is defined by

$$\sigma_{\text{accuracy}} = \frac{1}{N} \sum_{i=1}^{N} |R_i - R_{real}| \tag{8}$$

Where R_{real} is the real distance.

Fig. 2(a) shows the simulation of time histograms versus signal photoelectrons. In the figure, The position of the detected signal pulse drifts with the photoelectron number. As the number of photoelectrons increases, the width of the pulse decreases. Ranging accuracy and ranging precision using the center-of-mass algorithm are shown independently in Fig. 2(b). The area selected by the

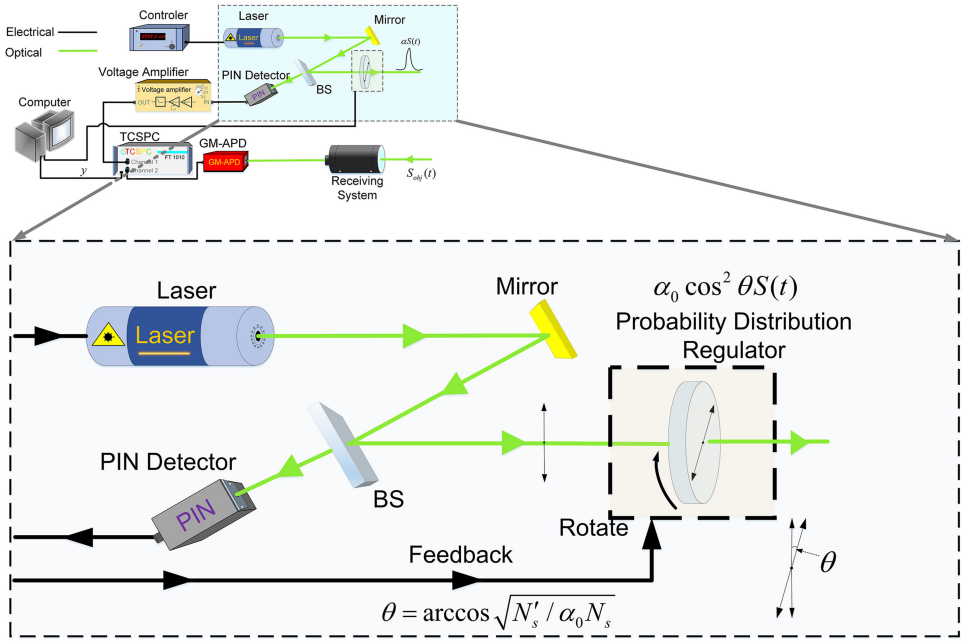

Fig. 3. Schematic of probability distribution regulator.

black dotted box in Fig. 2(b) is the area where the ranging accuracy is relatively high and the ranging precision is close to saturation.

3. Probability Distribution Regulator Method

3.1 Probability Distribution Regulator Theory

According to formula 4, the fluctuation of the number of photoelectrons will lead to the change of the detection probability distribution, and then causes the fluctuation of the range walk error. The range walk error can be actively controlled by limiting the number of photons before reaching the APD detector. Formula 2 points out that the total number of photoelectrons consists of the number of signal photoelectrons, background photoelectrons and dark counts of detectors. Therefore, a probability distribution regulator (PDR) is added before laser emission to limit the number of signal photons reaching the detector, so as to limit the total number of photoelectrons and achieve the desired effect of stabilizing the range walk error. We can select the number of photoelectrons that are limited by referring to the suitable area in Fig. 2(b).

A simple example of PDR is the controller whose attenuation coefficient varies with the number of incident photons of the detector. As shown in Fig. 3, a PDR based on a motor-driven rotating linear polarizer is presented. The minimum attenuation ratio of the polarizer is α_0. The angle between the polarization axis of linear polarizer and laser is θ. According to the Malus' law, the total attenuation ratio after the linear polarizer is $\alpha_0 \cos^2\theta$.

So the total attenuation rate can be controlled by adjusting the polarizer angle θ. The total attenuation rate of PDR is expressed as

$$\alpha = \frac{N'_s}{N_s} = \alpha_0 \cos^2\theta \tag{9}$$

Where N_s is the number of signal photoelectrons of APD detector. N'_s is the set number of signal photoelectrons of APD detector. The number of signal photons reaching the detector can be limited by adjusting the PDR polarizer angle θ to satisfy

$$\theta = \arccos\sqrt{N'_s / \alpha_0 N_s} \tag{10}$$

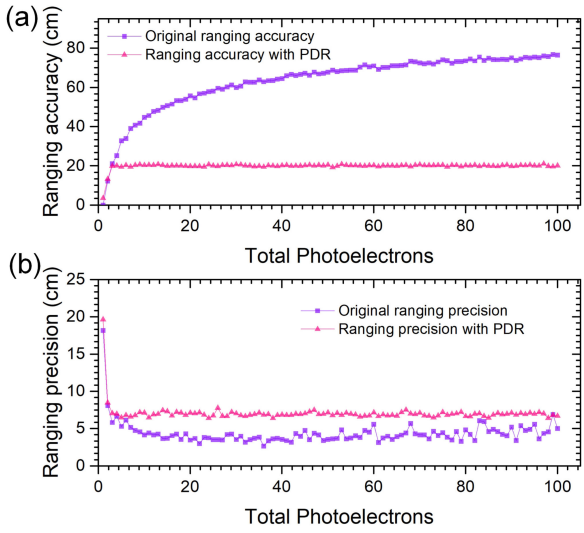

Fig. 4. Ranging accuracy and precision error versus total photoelectrons. (a) Without PDR. (b) Our method.

After adding the PDR, the photoelectrons number at time t is

$$N'_{sn}(t) = \alpha \frac{E_t}{h\nu} \frac{A_R}{2\pi R^2} \frac{\rho \eta_D \eta_R \cos\theta_R}{\sigma\sqrt{2\pi}} e^{-\frac{\left(t-\frac{2R}{c}\right)^2}{2\sigma^2}} + \eta_D N_b + N_d \tag{11}$$

Finally, the detection probability on the i-th time bin becomes

$$P'(i) = e^{-\sum_{j=1}^{i-1} N'_{sn}(j)} \left[1 - e^{-N'_{sn}(i)}\right] \tag{12}$$

3.2 Simulation Analysis

Combined with formula 5–9, the range walk error of photon counting lidar among the photoelectrons number is tested by simulations. Figs. 4 show the ranging accuracy and ranging precision versus total number of photoelectrons $N_{total} = \sum N_{sn}(i)$. Laser wavelength is 532 nm, the period is 4 kHz, $\sigma = 8$ and the single pulse energy is 5 $h\nu$. h is Planck constant and ν is laser frequency. The detection efficiency, dead time and dark count of detector is 35%, 45ns and $N_d = 0.006$, respectively. Target reflectivity $\rho = 0.1$, depth $\mu = 2R/c = 750$ (the 750th time bin, c is light speed). The number of background noise photoelectrons $N_b = 0.006$. TCSPC time bin $\Delta t = 256$ps. Accumulating $m = 40$ laser pulses to obtain a time histogram.

In the fig. 4(a), the ranging accuracy decreases with the increase of total photoelectron number. Under center-of-mass method the ranging accuracy ranges from 0cm to 80 cm and ranging precision ranges from 4 cm to 18 cm. The ranging accuracy tends to be saturated at the number of photoelectrons equals 100. But ranging precision is saturated very early, when the number of photoelectrons equals 4. Figs. 4 also show the effect of PDR on range walk error. The number of photoelectrons received by detector is set to three. The PDR results are the same as that at the corresponding position without PDR. The ranging accuracy is stabilized at $\sigma_{\text{accuracy,com}} = 21.1$ cm and the ranging precision is stabilized at $\sigma_{\text{precision,com}} = 5.8$ cm. PDR maintains the system's range walk error well.

3.3 Automatic Feedback Strategy

PDR needs to automatically adjust its attenuation coefficient according to the signal photoelectron number of APD detector response. Therefore, before a measurement, the system needs to make

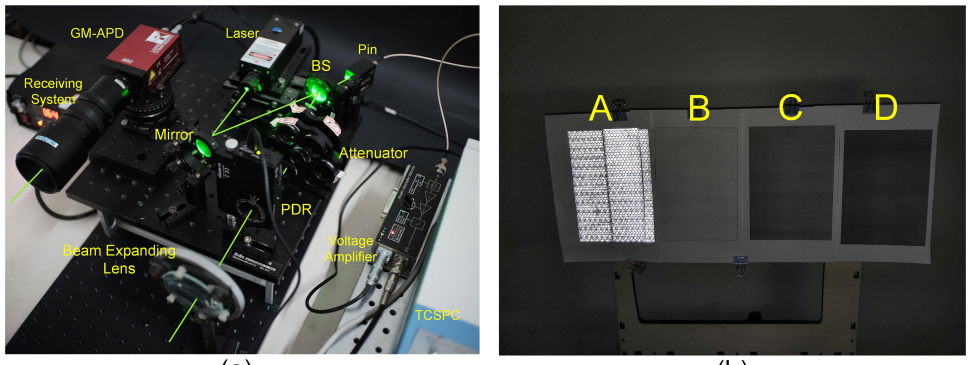

Fig. 5. Photograph of (a) the experimental setups and (b) the targets.

a short measurement, count the first N pulses of laser emission, to get the signal photoelectron number of APD detector when the polarization angle is at the initial position. There are six steps for a complete PDR measurement.

1) Rotate PDR polarization angle to the initial position.
2) Pre measurement: counting the first N laser pulses to obtain the signal photoelectron N_s of the APD detector.
3) Calculate the attenuation coefficient α according to the set number N'_s and the measured N_s using $\alpha = N'_s/N_s$.
4) Convert attenuation coefficient α to the angle θ that needs to rotate PDR.
5) Rotate PDR and complete the measurement of the current pixel.
6) Update pixel position and repeat step 1.

After adding PDR module, the increase of measurement time is mainly introduced by steps 1, 2 and 5. The increased response time of PDR method is given by formula (13). The time-consuming includes two rotations of the linear polarizer T_{rot} and pre measurement T_{pre} (calculating the rotation angle of polarizer by computer is ignored).

$$T_{resp} = 2T_{rot} + T_{pre} = \frac{2\arccos\sqrt{N'_s/\alpha_0 N_s}}{V_\theta} + N\,T_{laser} \tag{13}$$

Where N_s is the number of signal photoelectrons of APD detector. N'_s is the set number of signal photoelectrons of APD detector. V_θ is mean rotation speed of the linear polarizer, N is number of laser pulses in pre measurement, T_{laser} is the period of the laser. When the attenuation coefficient is from the minimum to the maximum, the polarizer only needs to rotate the angle $\pi/2$ at most, so the total time consumption for the rotating PDR is not greater than $\pi/V_\theta + N\,T_{laser}$.

4. Experiment and Analysis

For the experimental proof of our method, we established the photon counting lidar system with PDR, as shown in Fig. 5(a). we used a pulsed laser with 532 nm peak wavelength, 2ns pulse width, 4 kHz repetition frequency and 5 μJ single pulse energy. The GM-APD is a free-running Si SPAD (Laser Component, COUNT-100C) with a time jitter of about 1ns, a dead time of 45 ns, a detection efficiency of 55% and a dark count rate of 100 Hz. A TCSPC unit (SIMINICS, FT1010) is used to build up time histogram with 64 ps width of time bin. A receiving system (NAVITAR, ZOOM 7000, aperture diameter 5cm) with 79% transmittance at 532 nm is adopted to collect the echo signal from target. PDR consists of a Thorlab LPVISA100 linear polarizer and a stepper motor rotation mount K10CR1/M.

The objects used in the experiment are 4 paper with different reflection rates. Reflectivity decreases from A to D. Target A is attached with a retroreflector sticker. Target B, C, D are papers

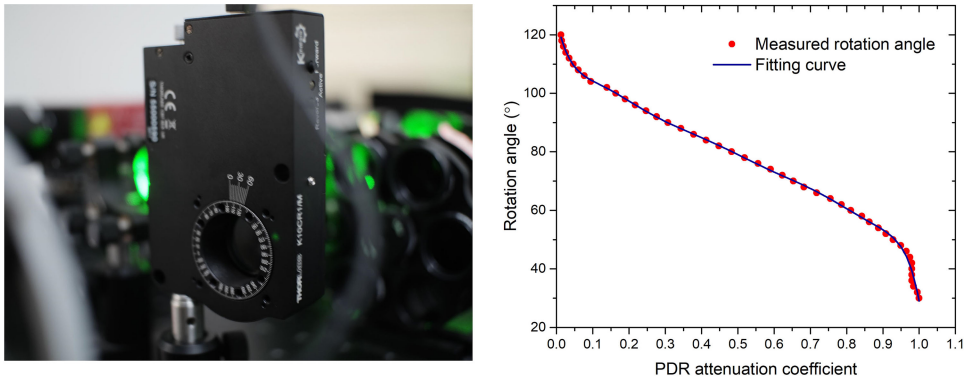

Fig. 6. (a) Photograph of the PDR. (b) PDR rotation angle versus PDR attenuation coefficient.

with incremental gray values. Each target has a size of 11 cm $\times$ 15.5 cm and is located 6.3m away. The laser beam is extended by a lens and illuminated on the target with a diameter of 5 cm.

Fig. 6(a) is a photograph of the PDR module used in the experiment. In step 4 of automatic feedback strategy, the rotation angle corresponding to the PDR needs to be quickly obtained according to the calculated attenuation coefficient. Therefore, we have previously calibrated the attenuation coefficient and rotation angle of the PDR module, as shown in Fig. 6(b). The function of PDR's rotation angle and attenuation coefficient is obtained by polynomial fitting with the measured value. So in step 4, we can quickly calculate the rotation angle of PDR through the attenuation coefficient. The PDR uses a high-precision stepper motor module with a rotation speed of 10 °/s. The pre measurement time is 0.2 s, and the TCSPC accumulation time after PDR adjustment is 1s. Since our experiment system only initially implements the PDR function, after the replacement of the liquid crystal polarizer or other nonlinear effect device and the replacement of the real-time TCSPC module will significantly reduce the response time of the PDR. For example, the rotation speed of a liquid crystal polarizer can reach 1500 °/s, which is 150 times faster than our PDR system.

Conventional method produces a series of ranging results in which the range walk error varies with the target reflectance as depicted in Figs. 7(A)–(c). Each target has been ranging 1600 times after one PDR adjustment, and each group of time histogram consists of 40 laser pulses emitted. The depth image of each target consists of 40 $\times$ 40 measured range values. The average power of laser emission is 300 μW. In the absence of PDR, the range walk error of each target is affected by reflectivity. After using PDR, the number of photoelectrons are controlled to six. In Fig. 7 (A)–(c), the ranging accuracy of A, B, C D are $\sigma_{\text{accuracy,com}} = 28.6$ cm, 7.4 cm, 3.6 cm, 1.6 cm, respectively. And the ranging precision are $\sigma_{\text{precision,com}} = 0.8$ cm, 1.5 cm, 1.7 cm, 2.0 cm. As depicted in Fig. 7(b)–(d), after using PDR to control the photoelectric number, the ranging accuracy and precision become $\sigma_{\text{accuracy,com}} = 3.2$ cm, 2.4 cm, 1.7 cm, 2.0 cm and $\sigma_{\text{precision,com}} = 2.1$ cm, 2.0 cm, 2.0 cm, 2.2 cm. The ranging accuracy increased by 8.9 times and ranging precision decreased by 2.6 times at most. For center-of-mass method, the standard deviation of ranging accuracy decreases from 12.43 cm to 0.65 cm, and standard deviation of ranging precision decreases from 0.51 cm to 0.1 cm. PDR effectively improves the ranging accuracy. Although the ranging precision is slightly deteriorated, the standard deviation of ranging accuracy and precision are reduced successfully. Therefore, the PDR method guarantees the range walk error stability well.

In order to explore the influence of background light on PDR method, we measured B and D objects without ambient light (average counting rate at about 0.023 counts/s for each time bin) and with ambient light ($\sim$0.456 counts/s for each time bin), as shown in Figs. 8. B' and D' represent the measurement results of B and D objects with ambient light. Each measurement of each target in this set of experiments was performed 49 times using the automatic feedback strategy for pre

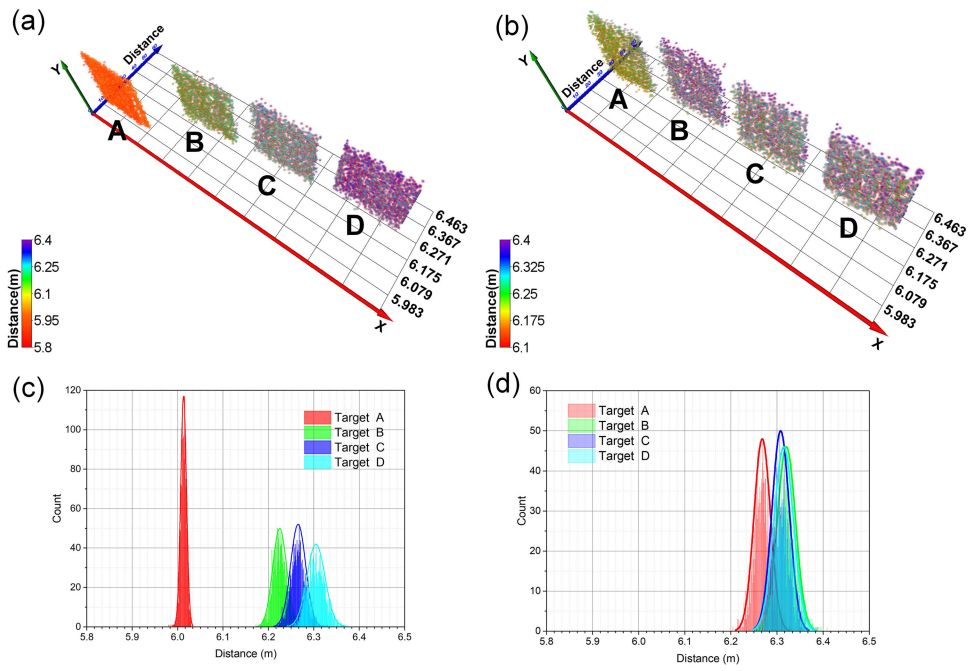

Fig. 7. (a) Depth image of conventional method with center-of-mass algorithm. (b) Depth image of proposed method with center-of-mass algorithm. (c) Distance histograms of (a). (d) Distance histograms of (b).

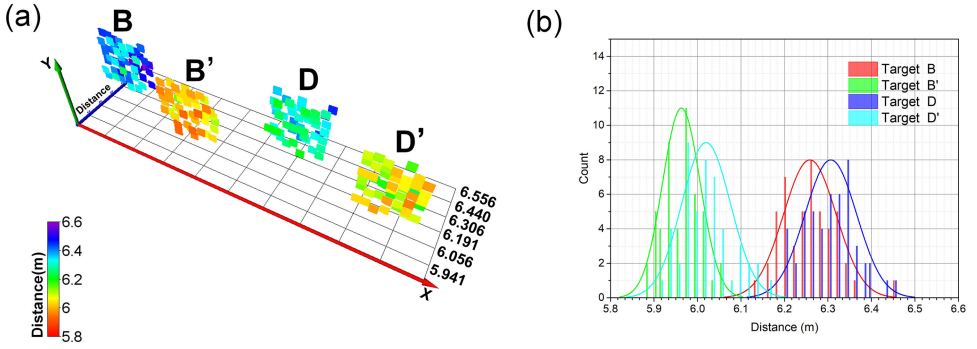

Fig. 8. (a) Depth image of conventional method with center-of-mass algorithm. (b) Distance histograms of (a).

measurement and attenuation adjustments. The total measurement time are 369.5s, 319.9s, 338.5s and 298.8s, respectively. The ranging accuracy of B, B', D, D' are $\sigma_{\text{accuracy,com}} =$ 4 cm, 34 cm, 1 cm, 28 cm. Under the influence of ambient light, the overall positions of B' and D' move forward. Although ranging error is improved by the presence of noise., PDR method effectively guarantees the standard deviation of accuracy error between different reflectance targets. The reason for the increase of ranging error can be explained by the Poisson model of single photon detection. As shown in formula (4), the detection probability of the laser signal decreases with the increase of background noise. If the set number of signal photoelectrons N_s' is not dynamically corrected, the number of photons actually emitted from the PDR will be more than the predetermined one, which will eventually lead to an increase in the accuracy error. In this case, combining our PDR method and previous methods to reduce ranging error, we can not only reduce the mean value of ranging error, but also ensure the stability of ranging error. In addition, we can continue to optimize the PDR

system strategy, dynamically adjust the set number of photoelectron N'_s to intelligently cope with ambient light noise.

4. Conclusion

In summary, a new probability distribution regulator method is proposed to ensure the fixed number of photon incident on the GM-APD by adjusting the number of photons emitted by the system, so as to achieve the stability of the range walk error. The theoretical formulas for the rotation angle of PDR based on two linear polarizers and the number of photons emitted by the control system have been derived. The experimental results demonstrate PDR method effectively guarantees the stability of range walk error. The ranging accuracy increased by 8.9 times and ranging precision decreased by 2.6 times at most. Although the ranging precision is slightly deteriorated, the standard deviation of ranging accuracy and precision are reduced from 12.43 cm to 0.65 cm and from 0.51 cm to 0.10 cm, respectively. In the next step, we plan to design a more intelligent PDR. More factors will also be taken into account to achieve a robust ranging system with stable range walk error.

References

[1] V. Molebny and O. Steinvall, "Multi-dimensional laser radars," *Proc. SPIE*, vol. 9080, 2014, Art. no. 908002.
[2] B. Schwarz, "LIDAR: Mapping the world in 3D," *Nature Photon.*, vol. 4, no. 7, pp. 429–430, 2010.
[3] C. Mallet and F. Bretar, "Full-waveform topographic lidar: State-of-the-art," *ISPRS J. Photogrammetry Remote Sens.*, vol. 64, no. 1, pp. 1–16, 2009.
[4] A. Kirmani *et al.*, "First-photon imaging," *Science*, vol. 343, no. 6166, pp. 58–61, 2014.
[5] D. Shin *et al.*, "Photon-efficient imaging with a single-photon camera," *Nature Commun.*, vol. 7, 2016, Art. no. 12046.
[6] F. Wang, Y. Zhao, Y. Zhang, and X. Sun, "Range accuracy limitation of pulse ranging systems based on Geiger mode single-photon detectors," *Appl. Opt.*, vol. 49, no. 29, pp. 5561–5566, 2010.
[7] O. Steinvall and T. Chevalier, "Range accuracy and resolution for laser radars," *Proc. SPIE*, vol. 5988, 2005, Art. no. 598808.
[8] X. Li, B. Yang, X. Xie, D. Li, and L. Xu, "Influence of waveform characteristics on LiDAR ranging accuracy and precision," *Sensors, Basel*, vol. 18, no. 4, 2018, Art. no. 1156.
[9] L. Xu, Y. Zhang, Y. Zhang, C. Yang, X. Yang, and Y. Zhao, "Restraint of range walk error in a Geiger-mode avalanche photodiode lidar to acquire high-precision depth and intensity information," *Appl. Opt.*, vol. 55, no. 7, pp. 1683–1687, 2016.
[10] W. He, B. Sima, Y. Chen, H. Dai, Q. Chen, and G. Gu, "A correction method for range walk error in photon counting 3D imaging LIDAR," *Opt. Commun.*, vol. 308, pp. 211–217, 2013.
[11] L. Xu *et al.*, "Signal restoration method for restraining the range walk error of Geiger-mode avalanche photodiode lidar in acquiring a merged three-dimensional image," *Appl. Opt.*, vol. 56, no. 11, pp. 3059–3063, 2017.
[12] T. Ruotsalainen, P. Palojarvi, and J. Kostamovaara, "A wide dynamic range receiver channel for a pulsed time-of-flight laser radar," *IEEE J. Solid-State Circuits*, vol. 36, no. 8, pp. 1228–1238, Aug. 2001.
[13] G. Kirchner and F. Koidl, "Compensation of SPAD time-walk effects," *J. Opt. A, Pure Appl. Opt.*, vol. 1, no. 2, pp. 163–167, 1999.
[14] I. Rech, I. Labanca, M. Ghioni, and S. Cova, "Modified single photon counting modules for optimal timing performance," *Rev. Sci. Instrum.*, vol. 77, no. 3, 2006, Art. no. 33104.
[15] L. Ye, G. Gu, W. He, H. Dai, and Q. Chen, "A real-time restraint method for range walk error in 3-D imaging lidar via dual detection," *IEEE Photon. J.*, vol. 10, no. 2, pp. 1–9, Apr. 2018.
[16] S. Johnson, P. Gatt, and T. Nichols, "Analysis of Geiger-mode APD laser radars," *Proc. SPIE*, vol. 5086, 2003, pp. 359–368.